Potential scattering of electrons in the presence of intense laser fields using the Kramers-Henneberger transformation

R. Bhatt, B. Piraux, and K. Burnett
Blackett Laboratory, Imperial College, London SW7 2BZ, England
(Received 30 April 1987)

The Kramers-Henneberger transformation is used to treat potential scattering of electrons in the presence of a strong laser field. As a first step, the one-dimensional scattering by a polarization potential is considered. It is shown that the static part of the effective potential, often called the dressed potential, may support more bound states than the original potential depending on the intensity and frequency of the field. Exact results for the transmission and reflection coefficients are presented and two approximations are discussed: A perturbative approach based on the above transformation and the adiabatic approximation.

I. INTRODUCTION

The reasons for calculating charged-particle scattering in an intense laser field are many and varied. This process plays an important role in areas such as plasma physics and also atomic physics, where it allows the observation of new resonances. This variety of motivations has stimulated a lot of theoretical studies starting with the well-known Kroll and Watson[1] work on the soft-photon approximation. Perturbative treatments[2–6] abound but their range of validity remains to be clearly established. To the best of our knowledge, the only existing nonperturbative approach has required a simplifying assumption about the potential,[7,8] namely, that it is separable. Recently, a new nonperturbative method based on the Kramers-Henneberger (KH) transformation[9,10] has been proposed by Gavrila and Kaminski.[11] Their work suggests that this transformation might be particularly useful in the case of intense high-frequency fields where an expansion of the scattering amplitude in inverse powers of the Laser frequency is reasonable.

The motivation for this work is quite simple: It is to test the scheme of Gavrila and Kaminski and also to consider some more general aspects of potential scattering using the KH transformation. When linearly polarized light is considered, as in our case, the problem "reduces" to the solution of an infinite system of coupled (two-dimensional) second-order differential equations. A complete numerical solution of this problem is therefore very complicated; so, we decided, as a first step, to restrict our treatment to one dimension. Although this simplification seems unrealistic, it nevertheless allows us to test several approximations within this approach and, we believe, provides information about the number of equations we have to take into account.

Section I of this paper is devoted to a brief outline of the general method. In Sec. II we apply this method to one-dimensional scattering of electrons by a polarization potential; the transformed potential and in particular its static part, usually called the dressed potential, are analyzed in detail. It is shown that the dressed potential may contain, depending on the laser parameters, more bound states than the undressed potential. This new feature may lead to new laser-induced resonances in the scattering cross section. In Sec. III we present results for the reflection and transmission coefficients and test the assertion of Gavrila and Kaminski, namely, the existence, in the high-frequency limit, of an iterative solution of the Schrödinger equation in the transformed representation. It is shown that this assertion, within our model, must be treated with due care and attention; in fact, if the limits delineated by Gavrila and Kaminski are strictly observed the iterative solution is a reasonable approximation to the full wave function. We have also tested the adiabatic approximation; this approximation is shown to be inadequate except at very high frequency when the coupling between the elastic and inelastic channels is weak.

II. THE MODEL

We consider the scattering of an electron by a polarization potential of the form

$$V(r)=\frac{-A}{(\beta^2+r^2)^2}\ , \tag{1}$$

where A is the potential strength and β is chosen arbitrarily (but different from zero). The scattering occurs in the presence of a strong laser field. This field is treated classically within the dipole approximation as a monochromatic infinite plane wave linearly polarized along the incident direction of the electron,

$$\mathbf{E}(t)=\mathbf{E}_0\sin(\omega t)\ . \tag{2}$$

The dynamics of the system are governed by the Schrödinger equation

$$i\hbar\frac{\partial\Psi}{\partial t}(\mathbf{r},t)=\left[\frac{1}{2m}[-i\hbar\nabla-q\,\mathbf{A}(t)]^2+V(r)\right]\Psi(\mathbf{r},t)\ , \tag{3}$$

where m and q are the mass and charge, respectively, of the electron. $\mathbf{A}(t)$ is the vector potential,

$$\mathbf{A}(t)=\mathbf{A}_0\cos(\omega t)\ . \tag{4}$$

Let us now introduce the new wave function[10]

$$\Phi(\mathbf{r},t)=U_1U_2\Psi(\mathbf{r},t)\ , \tag{5}$$

where

$$U_1=\exp\left[\frac{iq^2}{2mh}\int_{-\infty}^{t}d\tau\ \mathbf{A}^2(\tau)\right]\ , \tag{6}$$

$$U_2=\exp\left[\frac{-q}{m}\int_{-\infty}^{t}d\tau\ \mathbf{A}(\tau)\cdot\nabla\right]\ . \tag{7}$$

U_1 is the usual phase transformation which removes the A^2 term from the Schrödinger equation (3) while U_2 is the so-called "space-translation" transformation originally proposed by Kramers.[9] The physical meaning of the latter transformation has been discussed in detail by Henneberger.[10] It is usually written as

$$U_2=\exp(\boldsymbol{\alpha}\cdot\nabla)\ , \tag{8}$$

where

$$\boldsymbol{\alpha}=\boldsymbol{\alpha}_0\sin(\omega t),\quad \boldsymbol{\alpha}_0=-q\,\mathbf{A}_0/m\omega\ . \tag{9}$$

The new wave function satisfies the following differential equation:

$$i\hbar\frac{\partial\Phi}{\partial t}(\mathbf{r},t)=\left[\frac{-\hbar^2}{2m}\nabla^2+V(\mathbf{r}+\boldsymbol{\alpha}(t))\right]\Phi(\mathbf{r},t)\ . \tag{10}$$

As is clear from Eq. (10), the introduction of the electric field (2) transforms the spherical symmetry of the problem into a cylindrical symmetry; as a result, the field mixes states of different angular momentum, which greatly complicates the numerical calculations. Therefore, keeping in mind the purpose of this paper, we work as a first step in a one-dimensional space and consider the following equation (from now on we use atomic units except where stated):

$$i\partial\Phi(x,t)/\partial t=\left[-\frac{1}{2}\frac{\partial^2}{\partial x^2}+V(x+\alpha(t))\right]\Phi(x,t)\ . \tag{11}$$

In order to solve Eq. (11) numerically, we follow the procedure proposed by Gavrila and Kaminski. Since the potential is a periodic function of time, we use the Floquet theorem and seek a solution of the form

$$\Phi(x,t)=e^{-iE_it}\sum_{n=-\infty}^{+\infty}\phi_n(x)e^{-in\omega t}\ . \tag{12}$$

We also Fourier analyze the potential,

$$V(x+\alpha(t))=\sum_{n=-\infty}^{+\infty}V_n(\alpha_0;x)e^{-in\omega t}\ . \tag{13}$$

The Fourier components can be written as

$$V_n(\alpha_0;x)=-A\frac{i^n}{\pi}\int_0^{\pi}d\vartheta\frac{\cos(n\vartheta)}{[\beta^2+(x+\alpha_0\cos\vartheta)^2]^2}\ , \tag{14}$$

where we take (1) into account. By inserting (12) and (13) into (11) we get an infinite system of coupled differential equations for the components $\phi_n(x)$,

$$-\frac{1}{2}\frac{d^2}{dx^2}\phi_n+[V_0-(E_i+n\omega)]\phi_n+\sum_{\substack{m=-\infty\\(m\neq n)}}^{+\infty}V_{n-m}\phi_m=0\ . \tag{15}$$

In practice, this system of equations has to be truncated to N equations. Introducing $-n_e$ (≤ 0) and n_a (≥ 0), the lower and upper limits of N, respectively, we can write N as

$$N=n_e+n_a+1\ . \tag{16}$$

The choice of the value of n_e and n_a is discussed in detail in Sec. III. The boundary conditions of the problem are a flux of particles of energy E_i and momentum $k_i=\sqrt{(2E_i)}$ in the incoming channel and a flux of scattered particles of energy $E_n=E_i+n\omega$ and momentum $k_n=\sqrt{(2E_n)}$ in the outgoing channel n, where $n=0,\pm1,\pm2,\ldots$. When $E_n\geq 0$, the outgoing channel is open and when $E_n<0$ it is closed. The solution of the system (15) provides the reflection and transmission coefficients r_n and t_n, respectively, in channel n; these coefficients as well as the method used to calculate them are discussed in the Appendix.

Before analyzing the solution of the system (15), let us first examine in detail the zeroth-order Fourier component $V_0(\alpha_0;x)$, which is the time average of the potential in Eq. (11) and is often called the "dressed" potential. From Eq. (14), we get after some manipulation

$$V_0(\alpha_0;x)=\frac{-A}{2\beta^3}\mathrm{Re}\left[\frac{2\beta^2-x^2+\alpha_0^2+3i\beta x}{[(\beta+ix)^2+\alpha_0^2]^{3/2}}\right]\ . \tag{17}$$

Figure 1 shows $V_0(\alpha_0;x)$ as a function of x for various values of α_0 and unit values of A and β. The presence of the two minima at $x\simeq\pm\alpha_0$ reflects the fact that classically the charge responsible for the potential (1) appears to oscillate in the KH picture with an amplitude α_0, staying longer at the end points than in the middle where it gives rise to a weaker potential. In Fig. 2 we

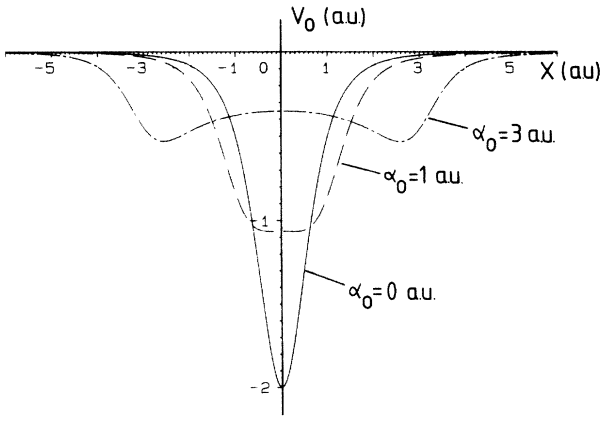

FIG. 1. Plot of the dressed potential $V_0(\alpha_0;x)$ as a function of x for $\alpha_0=0,1,3$ a.u. The potential parameters A and β are equal to 1 a.u.

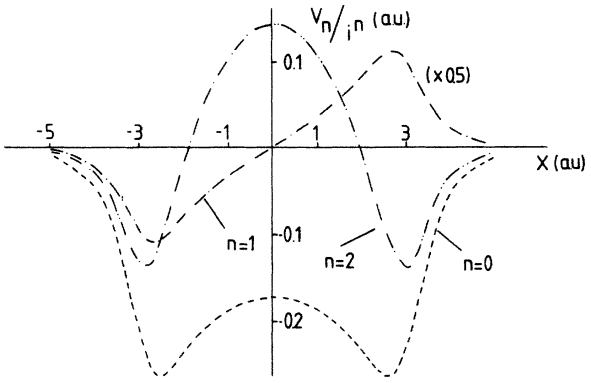

FIG. 2. Plot of V_n $(\alpha_0/x)i^n$ $(n=0,1,2)$, the first terms in the Fourier expansion of the potential V, as a function of x for $\alpha_0=3$ a.u.

compare $V_0(\alpha_0;x)$ with $V_n(\alpha_0;x)/i^n$ $(n=1,2)$ for $\alpha_0=3$ a.u. A striking fact which is evident from this figure is that the magnitude of the higher-order components is similar to that of $V_0(\alpha_0;x)$ except for large values $|x| \gg \alpha_0$, in which case we have

$$V_n(\alpha_0,x) \underset{x\gg\alpha_0}{\propto} \frac{-A\alpha_0^n}{n!x^{4+n}} . \tag{18}$$

This similarity in magnitude indicates that one must be cautious in treating the first few V_n $(n\neq 0)$ perturbatively. Section III will throw more light on this point. It is also interesting to analyze the energy levels of V_0. These levels are, in the high-frequency limit, the dressed levels of the atom in the presence of the field.[12] At lower frequencies, however, it is necessary to include the effect of the time-dependent part of the potential[13]. In Fig. 3 the energy levels of V_0 are plotted as a function of α_0. For $\alpha_0=0$ (field-free case) V_0 reduces to V, which in this particular case ($A=1$ a.u. and $\beta=1$ a.u.) supports only one bound state. When the field is switched on, this level moves upwards, as expected, since V_0 becomes more shallow. Furthermore, as α_0 increases, new bound states appear; the behavior of these is totally different from that of the ground state: They become more and more bound with increasing α_0 until a particular value of α_0, when they start to move upwards like the ground state. Although the appearance of the new bound states may seem surprising at first sight, given that the depth of the potential decreases with α_0, we must remember that the number of bound states also depends on the range of the

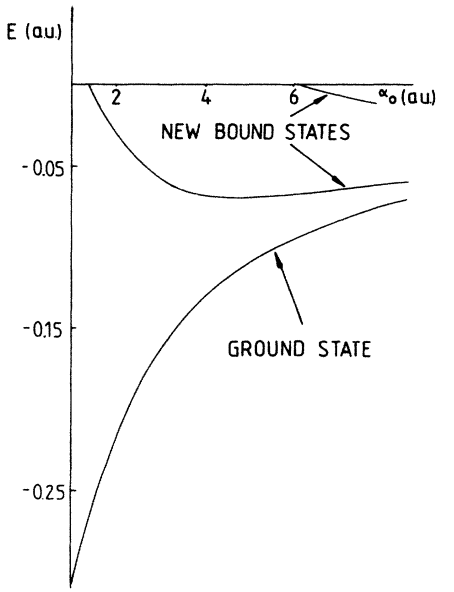

FIG. 3. Behavior of the energy levels of the dressed potential V_0 as a function of α_0. The potential parameters A and β are equal to 1 a.u.; in this case, the potential V only supports one bound state at $E=-0.40$ a.u.

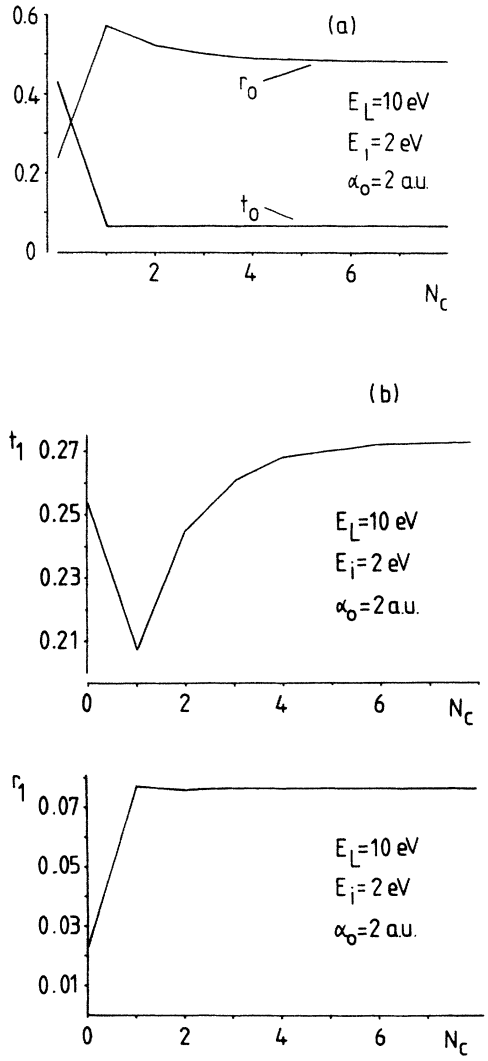

FIG. 4. Plot of the reflection and transmission coefficients r_n and t_n as a function of N_c, the number of closed channels for (a) $n=0$ corresponding to the elastic channel and (b) $n=1$ corresponding to the channel in which one photon has been absorbed. The other parameters are $E_L=10$ eV, $\alpha_0=2$ a.u., and $E_i=2$ eV; A and β are equal to 1 a.u. and the number of open channels is kept fixed at 17.

potential. For high values of α_0 the range of V_0, essentially determined by α_0, increases; when this effect is dominant, it is conceivable that new bound states may appear, as in our case.

III. RESULTS AND DISCUSSION

To what extent may perturbation theory be used to treat the high-order Fourier components of the potential (13), in particular at high frequencies? In the absence of a general rule that answers this question, we chose to investigate how many channels have to be included in solving the system (15) numerically for various values of the laser parameters α_0 and ω.

Consider first Fig. 4, which shows r_0, t_0, r_1, t_1 as functions of N_c, the number of closed channels included in the calculations (the number of open channels is fixed and equal to 17) for the case where the photon energy $E_L = 10$ eV, $\alpha_0 = 2$ a.u., $A = 1$ a.u., $\beta = 1$ a.u., and $E_i = 2$ eV. Under these conditions, the photon energy is about twice the binding energy of the ground state of V_0. As we see from the figure, r_0 and t_0 become stable after the inclusion of three closed channels while r_1 and, in particular, t_1 require more than five closed channels to become stabilized. The main point which emerges from this result is that channels whose energy is far below the ground state of V_0 are important; in other words, it is clear that the first Fourier components of the potential, V_{-1}, V_{-2}, cannot be treated as perturbations.

We can contrast this with the situation where E_L is much greater than the binding energy of the ground state denoted by E_0 (α_0) and the incident energy of the electron. As shown in Fig. 5(a), where $E_L = 6$ eV, $E_0 = -0.25$ eV, $E_i = 0.5$ eV, and $\alpha_0 = 10$ a.u., we find that the total number of contributing channels is about nine (five open and four closed channels), i.e., significantly reduced compared with around 23 for the previous case. In addition, it is clear that the inclusion of the first coupling terms $V_{\pm 1}, V_{\pm 2}$ only affects t_0 and r_0 by less than 10%. We therefore expect that a perturbative treatment of $V_{\pm 1}, V_{\pm 2}$, etc., is reasonable. Let us note that in this case the "Gavrila-Kaminski" conditions (namely, $E_L \gg |E_0|$, $E_L \gg E_i$, $\alpha_0^2 \omega \gg 1$) are fulfilled. However, if the potential is sufficiently strong (but still satisfying the condition $E_L \gg E_0$), the incident electron may feel the structure of the potential strongly by virtual emission of one photon ($E_i + E_0 \sim E_L$); in that case, shown in Fig. 5(b), the number of channels to be taken

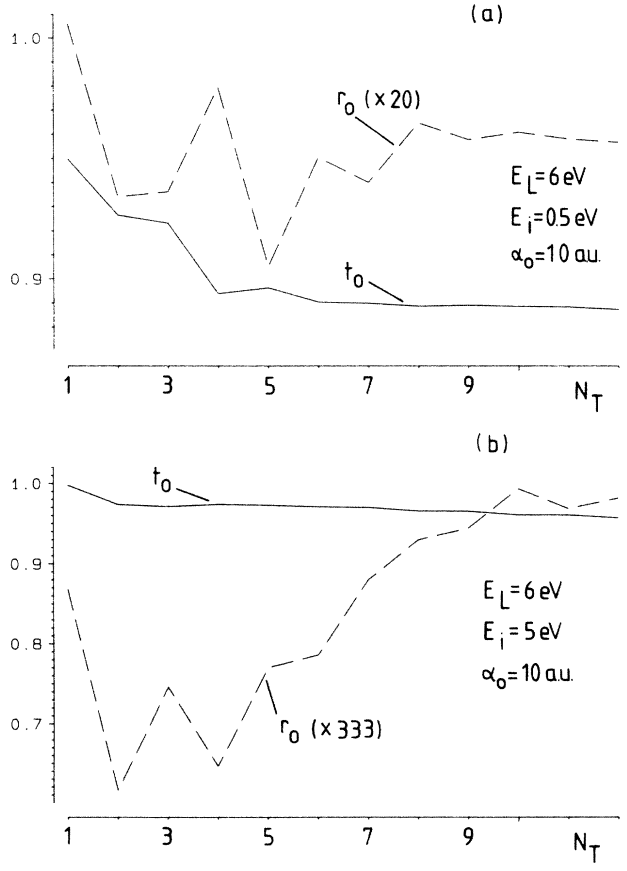

FIG. 5. Plot of r_0 and t_0 as functions of N_T, the total number of channels, for the case $E_L = 6$ eV, $\alpha_0 = 10$ a.u. and the incident energy is (a) $E_i = 0.5$ eV and (b) $E_i = 5$ eV; $A = 0.2$ a.u. and $\beta = 1$ a.u.

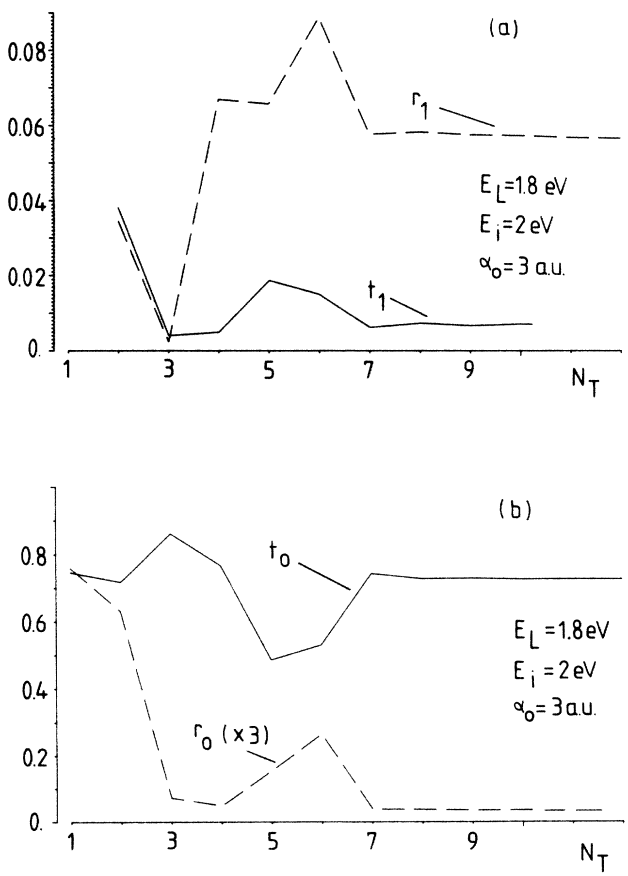

FIG. 6. Plot of (a) r_0 and t_0; (b) r_1 and t_1 as functions of N_T, the total number of channels, for the case $E_L = 1.8$ eV, $\alpha_0 = 3$ a.u., and $E_i = 2$ eV; A and β are equal to 1 a.u.

into account increases for the calculation of the reflection coefficients. In Fig. 6(a), we consider the case $E_L = 1.8$ eV, $\alpha_0 = 3$ a.u., $E_i = 2$ eV; as may be seen from the figure, the first Fourier components $V_{\pm 1}, V_{\pm 2}, V_{\pm 3}$ must be treated exact while the others, $V_{\pm |n|}, |n| > 3$, could be treated perturbatively. In conclusion, these results strongly suggest that perturbation theory applies only for very high frequencies and high α_0 requiring strong fields which, at present, have yet to be achieved experimentally.

Let us now analyze the reflection and transmission coefficients r_n and t_n, respectively. We first consider the case $E_L = 1.8$ eV and $\alpha_0 = 3$ a.u. Figure 7 shows t_0 and r_0 as functions of the incident energy. These results confirm the previous discussion and demonstrate that the above conclusions are valid for a wide range of incident energies. The presence of the cusps in t_0 corresponds each time to the opening of a closed channel. At this stage it is pertinent to ask what effect the presence of the new bound states might have on the transmission and reflection coefficients. For this particular value of α_0 (3 a.u.), V_0 supports two bound states of energy, $E_0 = -4.36$ eV and $E_1 = -1.59$ eV. We observe (see Fig. 8) a well-pronounced structure (in addition to the cusps already mentioned) in the behavior of $t_{\pm 1}$ and $r_{\pm 1}$ as a function of E_i. This structure is characterized by a sharp peak which occurs at $E_i \simeq 0.2$ eV for t_{+1} and $E_i \simeq 0.7$ eV for r_{+1}. It is hard to prove that this structure is a direct consequence of the presence of the new bound states. However, when α_0 decreases and reaches the critical value of about 1.2 a.u., for which there is only one bound state (see Fig. 3), the structure in t_{+1} disappears as shown in Fig. 9. It is also interesting to note that no resonance structure is present in the elastic channel. Figure 8 also shows that for this value of E_L (1.8 eV), $t_n(E_i) = t_{-n}(E_i + nE_L)$ and similarly for the reflection coefficients; further results prove that this is also true for larger n.

Finally, we present in Fig. 10 the behavior of t_0 and t_1 as functions of E_i for the case $E_L = 10$ eV and $\alpha_0 = 2$ a.u. It is interesting to note that at low incident energy, the total transmission coefficient is dominated by the inelastic contribution.

The numerical results have shown that straightforward perturbative expansion in V_n will not work except in the Gavrila-Kaminski regime mentioned above. We thought that it would be worthwhile to examine what is, in effect, the opposite of the perturbative limit when the coupling between the channels has a dominant effect. This may be studied by constructing the adiabatic states.

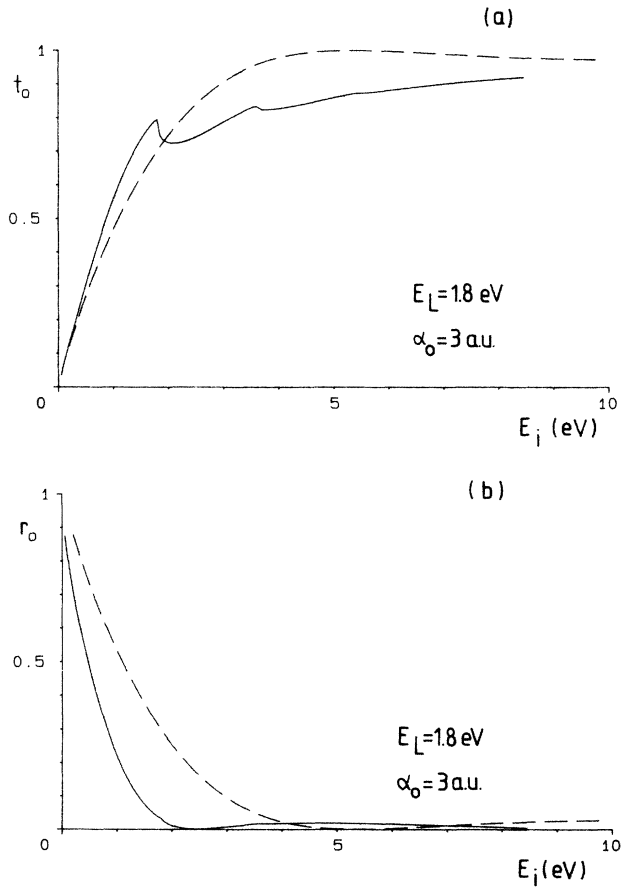

FIG. 7. Plot of (a) t_0 and (b) r_0 as functions of the incident energy E_i (in eV) for the case $E_L = 1.8$ eV and $\alpha_0 = 3$ a.u. — — —, one-channel calculation; ——, 20-channel calculation. A and β are equal to 1 a.u.

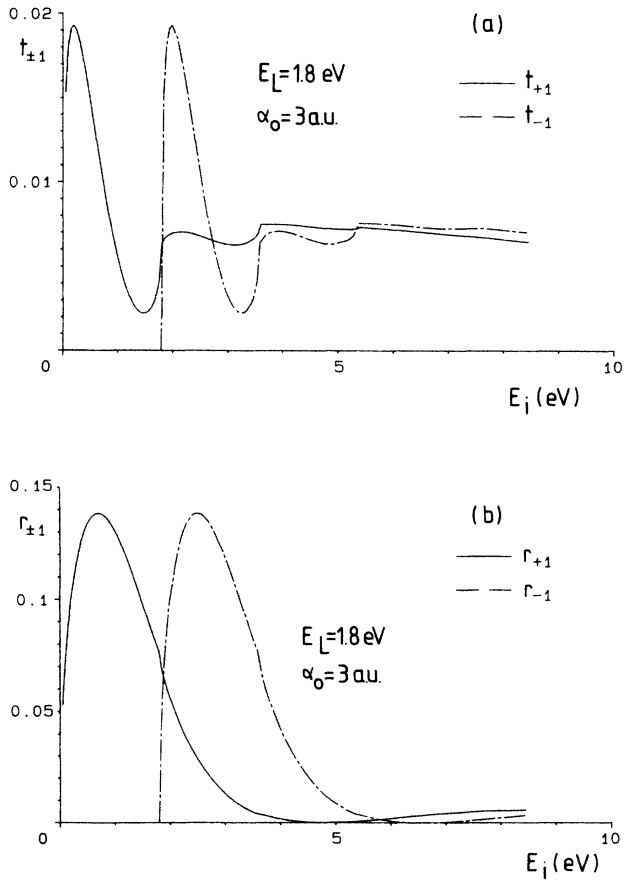

FIG. 8. Plot of (a) $t_{\pm 1}$ and (b) $r_{\pm 1}$ as functions of the incident energy E_i (in eV) for the case $E_L = 1.8$ eV, $\alpha_0 = 3$ a.u.; A and β are equal to 1 a.u.

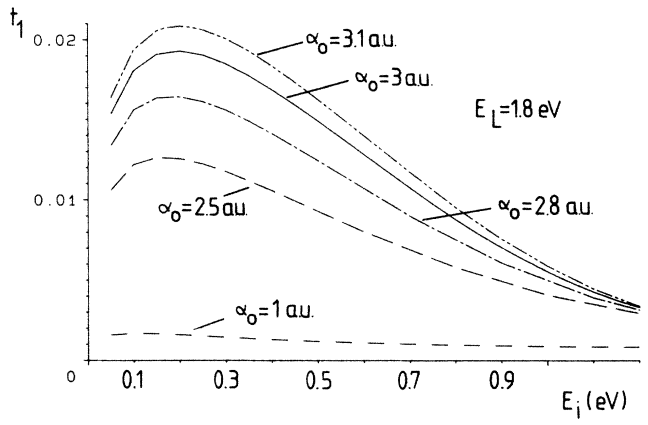

FIG. 9. Behavior of t_1 as a function of E_1 (in eV) for various values of α_0 (in a.u.) for the case $E_L = 1.8$ eV; A and β are equal to 1 a.u.

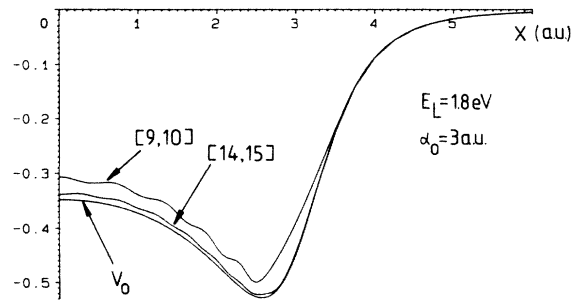

FIG. 11. Plot of the $n = 0$ adiabatic curves as a function of x for the case $\alpha_0 = 3$ a.u., $E_L = 1.8$ eV, and the potential parameters $A = 1$ and $\beta = 1$ a.u. The curves labeled by [9,10] and [14,15] have been calculated using 9 and 14 closed channels and 10 and 15 open channels, respectively, plus the elastic channel.

These states are obtained by removing the kinetic energy terms from the Hamiltonian and diagonalizing the remaining coupling matrix ($A2$ for $E_i = 0$) for each value of x. By doing this we find the set of potential curves that very-slow-moving electrons would "see." In the strict adiabatic limit where the velocity of the electron tends to zero, we ignore any coupling between these curves induced by the motion of the electron. An electron with vanishing speed would then "follow" one of the adiabatic curves. It was thought that these adiabatic curves would help us to understand the reflection and transmission coefficients. We argued that in the limit of very strong coupling the perturbation due to the kinetic energy terms would be small and we could think, e.g., of resonances as being due to the electron moving on a particular adiabatic curve. The form of the adiabatic curves we obtained appears to rule this out.

In Fig. 11 we have plotted the ($n = 0$) adiabatic curve for the case $\alpha_0 = 3$ a.u. and $E_L = 1.8$ eV. These curves have been constructed using, in addition to the elastic channel, nine closed and ten open channels for the first case and 14 closed and 15 open channels for the second case. We can see that as we increase the number of channels the adiabatic curves converge to V_0. This clearly shows that a very large number of channels is needed for convergence and confirms the participation of these channels in the coupling process. It also shows, more importantly, that the adiabatic curves have the same form as the uncoupled curve. In other words, the adiabatic approximation will be no better at describing resonance positions than the completely uncoupled states. We could investigate whether a perturbation scheme which uses the adiabatic states as a basis and treats the kinetic energy as a perturbation is a fruitful line to follow. We do not think this is worthwhile since the analysis would have to involve a full configuration-interaction treatment if it is to succeed. We should remember that it would have to generate considerable shifts and widths to achieve agreement with theory. Such a scheme holds little advantage over the full computation we have made. We would, therefore, suggest that adiabatic perturbation theory is not the way forward.

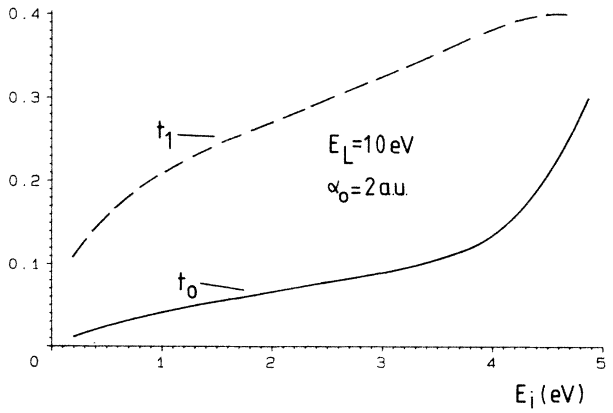

FIG. 10. Plot of t_0 and t_1 as functions of the incident energy E_i (in eV) for the case $E_L = 10$ eV, $\alpha_0 = 2$ a.u., and A and β are equal to 1 a.u.

ACKNOWLEDGMENTS

This work was supported in part by the U.K. Science and Engineering Research Council. One of us (R.B.) thanks the United Kingdom Atomic Energy Authority, Harwell, for additional support. We would also like to thank Dr. P. L. Knight and Dr. P. T. Greenland for stimulating discussions. One of us (B.P.) is particularly indebted to Dr. P. O'Mahony for illuminating conversations.

APPENDIX

In this appendix we describe in some detail the procedure adopted to calculate the reflection and transmission coefficients. We start by considering the system of

equations (15) truncated to N equations with N given by Eq. (16). For clarity, we use Greek latters for the index labeling the channel functions [the Fourier components of $\Phi(x,t)$]; in addition, this new index runs from 1 to N instead of $-n_e$ to n_a.

From the theory of differential equations, the homogeneous system (15) has a set of $2N$ linearly independent solutions. As a result, the channel function ϕ_λ is actually a linear combination of $2N$ functions, each denoted by $\chi_{\lambda,j}(1 \le j \le 2N)$. These $\chi_{\lambda,j}$ satisfy the following equation:

$$\frac{d^2}{dx^2}\chi_{\lambda,j} = \sum_\mu E_{\lambda,\mu}\chi_{\mu,j}, \quad 1 \le j \le 2N \ , \tag{A1}$$

where $E_{\lambda,\mu}$ is given by

$$E_{\lambda,\mu} = 2\{V_{\lambda-\mu} - \delta_{\lambda\mu}[E_i - (n_e - \lambda + 1)\omega]\} \ . \tag{A2}$$

In terms of the functions $\chi_{\lambda,j}$ the general solution may be written in matrix form as

$$\underline{\Phi}(x) = \begin{bmatrix} \chi_{1,1} & \cdots & \chi_{1,N} \\ \vdots & & \vdots \\ \chi_{N,1} & \cdots & \chi_{N,N} \end{bmatrix} \underline{A} + \begin{bmatrix} \chi_{1,N+1} & \cdots & \chi_{1,2N} \\ \vdots & & \vdots \\ \chi_{N,N+1} & \cdots & \chi_{N,2N} \end{bmatrix} \underline{B} \ , \tag{A3}$$

where $\underline{A}$ and $\underline{B}$ are constant $(N \times N)$ matrices. Using this notation, system (15) becomes

$$\underline{I}\frac{d^2}{dx^2}\underline{\Phi}(x) = \underline{E}(x)\underline{\Phi}(x) \ . \tag{A4}$$

$\underline{I}$ is the identity matrix and the elements of $\underline{E}$ are given by (A2).

We now suppose that the incident electron is moving from the right $(x = +\infty)$ towards the left $(x = -\infty)$. In addition, we assume that all the Fourier components $V_n(x)$ of the potential $V(x + \alpha\sin(\omega t))$ [see Eq. (18)] tend to zero faster than $1/x$ for large values of x. Under these conditions, the asymptotic behavior is

$$\underline{\Phi}(x) \underset{x \to -\infty}{\to} \begin{bmatrix} e^{-ik_1 x} & & & \\ & e^{-ik_2 x} & & 0 \\ & & \vdots & \\ 0 & & & e^{-ik_N x} \end{bmatrix} \underline{T} = \underline{K}^- \underline{T} \ , \tag{A5}$$

$$\underline{\Phi}(x) \underset{x \to +\infty}{\to} \begin{bmatrix} e^{-ik_1 x} & & & \\ & e^{-ik_2 x} & & 0 \\ & & \vdots & \\ 0 & & & e^{-ik_N x} \end{bmatrix} \underline{J} + \begin{bmatrix} e^{ik_1 x} & & & \\ & e^{ik_2 x} & & 0 \\ & & \vdots & \\ 0 & & & e^{ik_N x} \end{bmatrix} \underline{R} = \underline{K}^- \underline{J} + \underline{K}^+ \underline{R} \ . \tag{A6}$$

The wave vector k_n is defined by

$$k_n = \sqrt{(E_i + n\omega)}, \quad E_i + n\omega > 0 \tag{A7}$$

for an open channel and

$$k_n = i\sqrt{|E_i + n\omega|}, \quad E_i + n\omega < 0 \tag{A8}$$

for a closed channel. The elements of the $\underline{J}$ matrix are given by

$$J_{ij} = \delta_{n_e+1,i}\delta_{n_e+1,j} \ , \tag{A9}$$

reflecting the fact that the only incoming flux occurs in the channel corresponding to the energy E_i. $\underline{R}$ and $\underline{T}$ are the reflection and transmission matrices, respectively. We define the reflection and the transmission coefficients in channel λ as follows:

$$r_\lambda = \frac{k_\lambda}{k_{n_e+1}} |R_{\lambda,n_e+1}|^2 \ , \tag{A10}$$

$$t_\lambda = \frac{k_\lambda}{k_{n_e+1}} |T_{\lambda,n_e+1}|^2 \ . \tag{A11}$$

With this normalization, the conservation of probability is expressed as

$$\sum_\lambda (r_\lambda + t_\lambda) = 1 \ , \tag{A12}$$

where the sum over λ includes the open channels only.

In order to solve the system (A4) numerically, we adopt the following procedure: First, we divide the x axis into three intervals, $I_1 = (-\infty, -x_t)$, $I_2 = (-x_t, x_t)$, $I_3 = (x_t, +\infty)$. x_t, a positive number, is chosen such that the solution $\Phi(x)$ in the intervals I_1 and I_2 is given to a good approximation by the expressions (A5) and (A6), respectively. From Eq. (18), it is clear that x_t is essentially dependent on α_0. The second step consists of propagating numerically the solution $\Phi(x)$ from $x = -x_t$ to $x = +x_t$. At $x = -x_t$, the solution has the form (A5) but since at this stage we do not know the transmission matrix $\underline{T}$, we replace it by an arbitrary but nonzero matrix $\underline{B}$; thus,

$$\underline{\Phi}(x = -x_t) = \underline{K}^- \underline{B} \ . \tag{A13}$$

The numerical algorithm used in this calculation is based on the de Vogelaere method.[14]

At $x=x_t$, we require that the solution $\underline{\Phi}(x)$ and its first derivative $\underline{\Phi}'(x)$ be continuous. In other words, we have to find the constant matrix $\underline{A}$ such that

$$\underline{\Phi}(x_t)\underline{A}=\underline{K}^{-}\underline{J}+\underline{K}^{+}\underline{R} , \tag{A14}$$

$$\underline{\Phi}'(x_t)\underline{A}=\underline{K}^{-\prime}\underline{J}+\underline{K}^{+\prime}\underline{R} , \tag{A15}$$

where $\underline{K}^{+\prime}$ and $\underline{K}^{-\prime}$ are the first derivatives of $\underline{K}^{+}$ and $\underline{K}^{-}$, respectively. After trivial manipulation we obtain

$$\underline{R}=(\underline{\Phi}'^{-1}\underline{K}^{+\prime}+\underline{\Phi}^{-1}\underline{K}^{+})^{-1}(\underline{\Phi}^{-1}-\underline{\Phi}'^{-1})\underline{K}^{-}\underline{J} , \tag{A16}$$

$$\underline{A}=\underline{\Phi}^{-1}(\underline{K}^{-}\underline{J}+\underline{K}^{+}\underline{R}) , \tag{A17}$$

where as usual the superscript -1 denotes the inverse of a matrix. This procedure uniquely determines the reflection matrix $\underline{R}$ as well as the transmission matrix $\underline{T}$ given by

$$\underline{T}=\underline{B}\underline{A} . \tag{A18}$$

As a test of the computer code, we replace $\underline{E}(x)$ in (A2) by a constant matrix for which case the system can be solved analytically. In addition we also check, in each case presented here, the conservation of probability given by Eq. (A12).

---

[1]N. M. Kroll and K. M. Watson, Phys. Rev. A **8**, 804 (1973); for a review of the soft photon approximation see also L. Rosenberg, Adv. At. Mol. Phys. **18**, 1 (1982).

[2]J. I. Gersten and M. H. Mittleman, Phys. Rev. A **12**, 1840 (1975).

[3]M. H. Mittleman, Phys. Rev. A **19**, 134 (1978).

[4]G. Ferrante and C. Leone, Nuovo Cimento **48**, 35 (1978).

[5]G. Ferrante, C. Leone, and L. Lo. Cascio, J. Phys. B **12**, 2319 (1979).

[6]L. Rosenberg, Phys. Rev. A **34**, 4567 (1986).

[7]R. Shakeshaft, Phys. Rev. A **28**, 667 (1983).

[8]Another simplification might consist of using circularly polarized light, since in that case the problem can be made time independent by working in a rotating frame of reference; see also F. H. M. Faisal, Phys. Lett. A **119**, 375 (1987).

[9]H. A. Kramers, *Collected Scientific Papers* (North-Holland, Amsterdam, 1956), p. 272.

[10]W. C. Henneberger, Phys. Rev. Lett. **21**, 838 (1968).

[11]M. Gavrila and J. Z. Kaminski, Phys. Rev. Lett. **52**, 613 (1984).

[12]J. I. Gersten and M. H. Mittleman, J. Phys. B **9**, 2561 (1976).

[13]P. Lambropoulos, E. A. Power, and T. Thirunamachandram, Phys. Rev. A **14**, 1910 (1976).

[14]R. de Vogelaere, J. Res. Nat. Bur. Stand. **54**, 119 (1955).